Two-Photon Singlet Oxygen Sensitizers: Quantifying, Modeling, and Optimizing the Two-Photon Absorption Cross Section

Tina D. Poulsen,[†] Peter K. Frederiksen,[†] Mikkel Jørgensen,[‡] Kurt V. Mikkelsen,[§] and Peter R. Ogilby*[,†]

Department of Chemistry, Aarhus University, DK-8000 Århus, Denmark, Polymer Department, Risø National Laboratory, DK-4000 Roskilde, Denmark, and Department of Chemistry, University of Copenhagen, DK-2100 Copenhagen, Denmark

Received: May 22, 2001; In Final Form: September 13, 2001

Several substituted difuranonaphthalenes have been identified as being viable sensitizers for the production of singlet molecular oxygen ($a^1\Delta_g$) upon two-photon nonlinear excitation with a focused laser beam. The two-photon absorption cross sections of these molecules are comparatively large and depend significantly on the functional groups attached to the chromophore. To facilitate the further development of such sensitizers, computational tools have been employed to model the two-photon absorption cross sections of some difuranonaphthalenes as well as distyryl benzenes that likewise can be viable singlet oxygen precursors. Ab initio calculations using response theory yield cross sections that reproduce experimental data well. Specifically, for these comparatively large molecules, the calculations not only model relative substituent-dependent changes well but also yield reasonably accurate cross sections. Thus, ab initio computational methods can indeed be used as a predictive tool in the design of potentially useful, two-photon singlet oxygen sensitizers.

Introduction

Singlet molecular oxygen ($a^1\Delta_g$) is an intermediate in many oxidative degradation reactions and, as such, the photosensitized production of singlet oxygen has important ramifications in disciplines that range from photomedicine to polymer science.[1−4] In the plethora of sensitizer systems that have been studied over the past four decades, singlet oxygen has always been produced as a consequence of sensitizer excitation via a linear one-photon transition between the ground state, S_0, and a singlet excited state, S_n.[4] Although, in some sensitizers, singlet oxygen can be produced upon oxygen quenching of the sensitizer's lowest excited singlet state, S_1, singlet oxygen is generally produced more efficiently upon oxygen quenching of the sensitizer triplet state, T_1, formed upon intersystem crossing, $S_1 \rightarrow T_1$.

We have recently shown that singlet oxygen can also be produced and optically detected upon two-photon nonlinear excitation of a sensitizer with a focused laser beam.[5] In this case, the $S_0 \rightarrow S_n$ transition proceeds via a virtual state and follows selection rules[6] that differ from those for a one-photon transition. Rapid relaxation of the S_n state initially populated, however, yields S_1 which, in turn, should behave exactly as when formed via a one photon process. Thus, upon $S_1 \rightarrow T_1$ intersystem crossing, for example, oxygen quenching of T_1 will produce singlet oxygen in an overall yield that simply reflects the difference between the one- and two-photon absorption cross sections.[5]

The use of a two-photon nonlinear transition to populate an excited state of a given molecule has a number of attractive features.[6−9] For example, using a focused laser as the irradiation source imparts spatial resolution to an experiment and, thus, is pertinent in the construction of fluorescence microscopes.[7,8] Moreover, irradiation under conditions that preclude light absorption by the more dominant one-photon transitions facilitates depth penetration in samples that might otherwise be opaque. The latter can be useful in photodynamic therapy, for example, where tissue penetration is desired.[7,9] These attributes of pumping a two-photon transition are certainly pertinent to singlet oxygen production in that (1) the construction of a microscope capable of detecting singlet oxygen with spatial resolution could provide useful information on a variety of heterogeneous systems,[10] and (2) singlet oxygen can be a key reactive intermediate in the treatment of cancers using photodynamic therapy.[11]

To facilitate the further development and optimization of two-photon absorbers, including singlet oxygen sensitizers, it would be desirable to use computational tools to predict and model the expected behavior for a given molecule. An accurate computational method of assessing two-photon absorption cross sections, particularly for the comparatively large molecules usually desired, would certainly result in more efficient use of the often-limited resources available for the synthesis of such molecules.

Over the past few decades, a variety of approaches to computationally model two-photon absorption cross sections of organic molecules have been presented.[12−24] These approaches range from comparatively simple, approximate methods to more extensive and complicated ab initio methods, each characterized by specific advantages and disadvantages. Although semiempirical methods have recently been receiving a great deal of attention,[19,20] advances in a number of areas have made it possible to use more sophisticated ab initio methods,[25,26] even for comparatively large polyatomic systems.[21−24] For the present study, we set out to explore whether ab initio methods could be used to successfully model and ultimately predict nonlinear properties of viable singlet oxygen sensitizers.

* To whom correspondence should be addressed.
[†] Aarhus University.
[‡] Risø National Laboratory.
[§] University of Copenhagen.

10.1021/jp011974w CCC: $20.00
Published on Web 12/01/2001

CHART 1

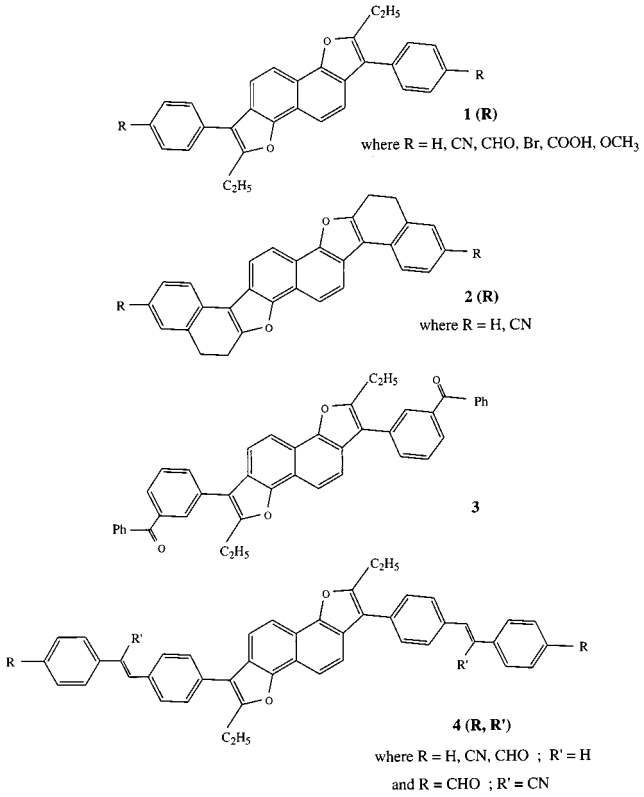

The two-photon absorption cross section can be determined from the imaginary part of the second order hyperpolarizability tensor at the two-photon resonance or by computing the individual two-photon transition matrix elements, $S_{\alpha,\beta}$.[7,23] One way of calculating these parameters is via a sum-over-states expression[7,14,19] in which all intermediate states, in principle, must be included. However, the traditional sum-over-states calculation can be problematic due to its slow convergence, the general requirement that a large number of terms must be included, and the need for explicit information about excited states (e.g., transition moments and energies).[14,27] On the other hand, response theory[28] provides an alternative and rigorous approach to investigate a number of molecular properties, including two-photon absorption cross sections. In this theory, the matrix elements describing the absorption of two photons are evaluated as the residues of the quadratic response functions containing the electric dipole operators. In this way, the time-consuming and approximate summation over states is avoided, but the exact sum-over-states value is implicitly obtained by solving a set of linear equations. Ågren and co-workers have demonstrated that response theory can indeed be a useful tool for calculating two-photon cross sections of reasonably large molecules.[21−24]

In the present study, we set out to use response theory to calculate two-photon absorption cross sections for a series of substituted difuranonaphthalenes (Chart 1) and distyryl benzenes (Chart 2). Experimental results indicate that the two-photon cross sections in these general classes of compounds depend significantly on the functional groups attached to the chromophore.[5,20] Moreover, we have also ascertained that selected difuranonaphthalenes and distyryl benzenes are, in fact, good two-photon singlet oxygen sensitizers.[5] Thus, these systems appear well suited to assess the accuracy and ease with which ab initio theory can be used to model and ultimately play a role in the development of more efficient two-photon singlet oxygen sensitizers.

CHART 2

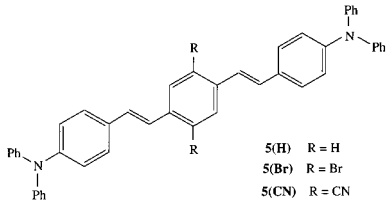

Experimental Section

Apparatus and Techniques. The methods we use to quantify two-photon absorption cross sections have been discussed in detail elsewhere.[5] Briefly, we use the photosensitized production of singlet oxygen to probe the efficiency of light absorption by the sensitizer in a two-photon process. In these experiments, the output of a nanosecond laser is focused into a solution of the sensitizer in toluene [Quanta-Ray GCR 230 Nd:YAG-pumped optical parametric oscillator (MOPO 710) or Nd:YAG pumped dye laser; pulse full width at half-maximum ∼5 ns, 10 Hz repetition rate]. The time-resolved 1270 nm phosphorescence of singlet oxygen [$O_2(a^1\Delta_g) \rightarrow O_2(X^3\Sigma_g^-)$] is then monitored from the laser beam focal point using a 77 K Ge detector [Edinburgh Instruments model EI−P, 400 ns response time]. The intensity of the singlet oxygen signal thus detected, normalized by the singlet oxygen quantum efficiency of that particular molecule, yields a parameter that is proportional to the two-photon absorption cross section. Absolute values for the cross section can be obtained by comparing these relative data to data similarly recorded from a sensitizer with a known two-photon absorption cross section. As the standard in our experiments, we use compound **5(Br)** (see Chart 2) for which a two-photon cross section at 800 nm of $(450 \pm 70) \times 10^{-50}$ cm^4 s $photon^{-1}$ has been reported by Albota et al.[20] and for which we have determined a singlet oxygen yield of 0.46 ± 0.05.[5] Laser intensities used in the two-photon experiments were typically in the range ∼10−15 mJ $pulse^{-1}$ cm^{-2}. Note that because the monochromatic output of a laser is simply focused into the sample, the photons absorbed in this nonlinear process have the same energy.

One-photon singlet oxygen yields were quantified by comparing the intensity of the 1270 nm singlet oxygen phosphorescence signal obtained from a given sensitizer to the signal observed upon irradiation of acridine, which has a singlet oxygen quantum yield of 0.83 ± 0.06 in toluene.

Upon irradiation, compound **4(CHO,H)** was not as stable as the other sensitizers used in our study. This instability was manifested by the creation of degradation products that gave rise to a background signal that, over time, eventually masked the singlet oxygen phosphorescence signal. Indeed, upon prolonged irradiation of a given sample of **4(CHO,H)** with a focused laser beam, a residue of carbon was ultimately deposited on the cuvette at the point where the beam entered the cell. Thus, to record the two-photon singlet oxygen data from **4-(CHO,H)**, it was necessary to flow or exchange the solution during the course of a given measurement (i.e., total exposure of ∼2000 laser pulses).

Sensitizer Preparation. With one exception, synthetic details for the molecules examined in our experimental work (Table 1, Charts 1 and 2) have likewise been published.[5,29] (Note: The difuranonaphthalenes synthesized for our experimental studies were prepared with pendant *n*-octyl groups to facilitate solubility in toluene. The calculations were performed on model analogues in which ethyl groups replaced the *n*-octyl groups.) For the present study, compound **4(CHO,H)** was prepared according

TABLE 1: Two-Photon Absorption Cross Sections for the Sensitizers Studied

sensitizer	one-photon singlet oxygen quantum yield	two-photon absorption cross section[a] ($\times 10^{50}$ cm^4 s photon^{-1}) expt	calc (3-21G)	calc (6-31G*)
1(H)	0.36 ± 0.04	8 ± 2[b]	7.0	7.0
1(CN)	0.36 ± 0.04	139 ± 35[b]	37	41
1(CHO)	0.49 ± 0.06	205 ± 50[b]	69	73
1(Br)	0.42 ± 0.05	7 ± 2[b]		
1(COOH)			58	61
1(OCH3)			0.6	1.2
2(H)	0.37 ± 0.04		5.6	6.0
2(CN)			34	39
3	0.67 ± 0.07	70 ± 30[b]	12	14
4(H,H)			7.6	9.2
4(CN,H)			111	126
4(CHO,H)	0.13 ± 0.01	780 ± 190[b]	123	136
4(CHO,CN)			129	
5(H)			165	122
5(Br)	0.46 ± 0.05	450 ± 70[c]	461	
5(CN)		1940 ± 290[d]	1040	930
pyrene	0.74 ± 0.07[e]	0.22[f]		0.08[g]

[a] Measured/calculated at the wavelengths indicated. [b] At 618 nm. [c] At 800 nm. From Albota et al.[20] [d] At 835 nm. From Albota et al.[20] [e] From Redmond and Braslavsky.[46] [f] At 694 nm. From Kershaw.[47] [g] Calculated using a g_{max} value of 2.77 × 10^{-14} s (see text).

SCHEME 1

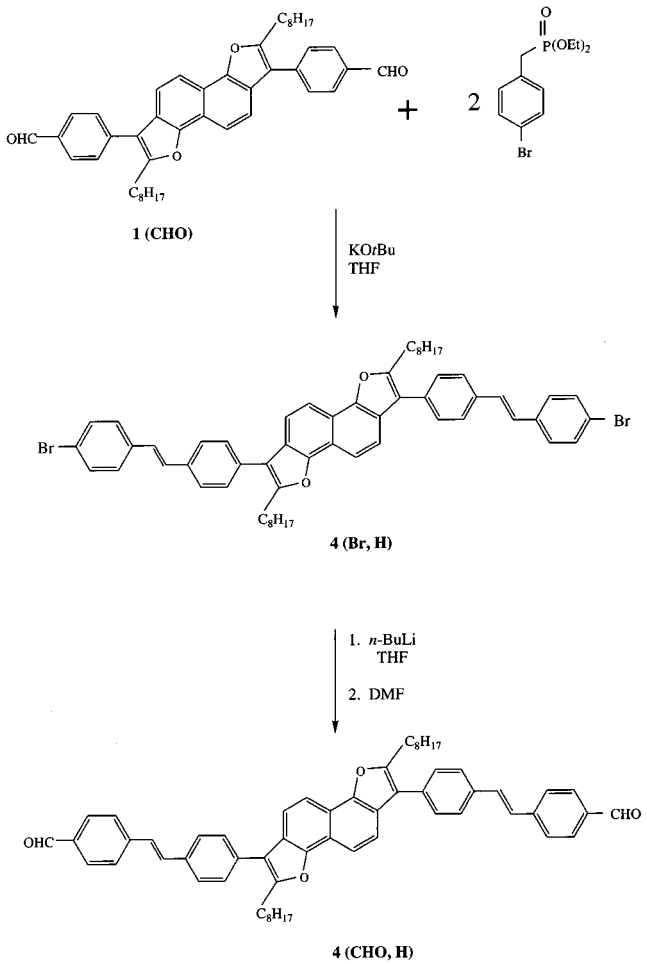

to the procedure outlined in Scheme 1. Briefly, compound **1-(CHO)** (3.2 g, 5 mmol) and diethyl 4-bromo-benzyl phosphonate ester[30] (3.1 g, 10 mmol) were dissolved in THF (50 mL) and condensed in a Horner-Emmons-Wadsworth reaction with potassium *tert*-butoxide (1.5 g, excess). The reaction mixture was heated to reflux for 30 min and then poured into ice water with dilute hydrochloric acid to precipitate the product. Recrystallization from toluene afforded compound **4(Br,H)** as an off-white crystalline powder. Yield: 3.23 g, 68%; mp: 228−30 °C. ^{1}H NMR (250.1 MHz, $CDCl_3$) δ: 0.88 (t, 6 H, *J* 7), 1.2−1.5 (m, 20 H), 1.89 (p, 4H, *J* 7), 2.99 (t, 4 H, *J* 7), 7.10 (d, 2H, *J* 16), 7.19 (d, 2H, *J* 16), 7.42 (d, 4H, *J* 8), 7.51 (d, 4H, *J* 8), 7.56 (d, 4H, *J* 8), 7.66 (d, 4H, *J* 8), 7.77 (d, 2H, *J* 9), 8.16 (d, 2H, *J* 9). ^{13}C NMR (62.9 MHz, $CDCl_3$) δ: 14.5, 23.1, 27.4, 29.2, 29.6, 29.7, 29.8, 32.3, 115.7, 118.2, 118.9, 119.1, 121.8, 123.8, 126.3, 127.4, 127.9, 128.4, 129.5, 129.9, 132.2, 133.2, 136.1, 136.7, 150.4, 155.0.

An X-ray structure determination of **4(Br,H)** indicates that the dihedral angle between the difuranonaphthyl core and the first phenyl of the pendant stilbenyl units is ∼41°. The stilbenyl units themselves are planar.

The dibromo compound **4(Br,H)** (1.0 g, 1.06 mmol) was dissolved in dry THF (25 mL) and, after cooling with a dry ice−acetone bath (−78 °C), *n*-BuLi (2 mL, 3.2 mmol) was added. The bromine-to-lithium exchange reaction was allowed to proceed for 10 min at low temperature, after which dimethyl formamide, DMF, (2 mL, excess) was added and the cooling bath removed. The reaction mixture was stirred for 1 h at ambient temperature and then dilute hydrochloric acid was added and the solvents removed in a vacuum. Recrystallization from heptane afforded compound **4(CHO,H)** as a yellow powder. Yield: 550 mg, 61%; mp 224−5 °C. ^{1}H NMR (250.1 MHz, $CDCl_3$) δ: 0.88 (t, 6H, *J* 6), 1.1−1.5 (m, 20H), 1.89 (p, 4H, *J* 7), 2.99 (t, 4H, *J* 7), 7.22 (d, 2H, *J* 16), 7.35 (d, 2H, *J* 16), 7.59 (d, 4H, *J* 8), 7.69 (dd, 8H, *J* 8), 7.77 (d, 2H, *J* 9), 7.89 (d, 4H, *J* 8), 8.17 (d, 2H, *J* 9). ^{13}C NMR (62.9 MHz, $CDCl_3$) δ: 14.5, 23.7, 27.5, 29.2, 29.6, 29.7, 29.8, 32.3, 115.8, 118.1, 118.9, 119.1, 123.7, 127.3, 127.8, 129.9, 130.7, 132.2, 133.8, 135.7, 135.8, 143.8, 150.4, 155.2, 192.0.

Computational Methods

General Background. Calculations were performed using the DALTON program package,[31] using response theory to obtain the two-photon absorption cross sections. The principal attribute of response theory is the possibility to obtain many molecular properties, including two-photon cross sections, in one calculation.[28] In the spectral representation, response functions contain summations over all intermediate states which, in turn, makes it possible to avoid problems associated with a traditional sum-over-states calculation. The response equations were solved as sets of coupled linear equations using iterative techniques and direct linear transformations. The two-photon cross sections were computed at the ab initio level in the random phase approximation that is equivalent to the time-dependent Hartree−Fock level. The matrix elements describing the absorption of two-photons were computed through a residue of the quadratic response function.[28]

The corresponding sum-over-states expression for the two-photon matrix elements, $S_{\alpha,\beta}$, can be written as[32]

$$S_{\alpha,\beta} = \sum_k \frac{\langle 0|\mu^\alpha|k\rangle\langle k|\mu^\beta|f\rangle}{\omega_k - \omega_f/2} + \frac{\langle 0|\mu^\beta|k\rangle\langle k|\mu^\alpha|f\rangle}{\omega_k - \omega_f/2} \qquad (1)$$

for the absorption of two photons of identical energy. In eq 1, ω_k denotes the excitation energy of the virtual intermediate state, $|k\rangle$, ω_f denotes the excitation energy of the final state, $|f\rangle$, μ^α and μ^β are electric dipole operators, and the summation is

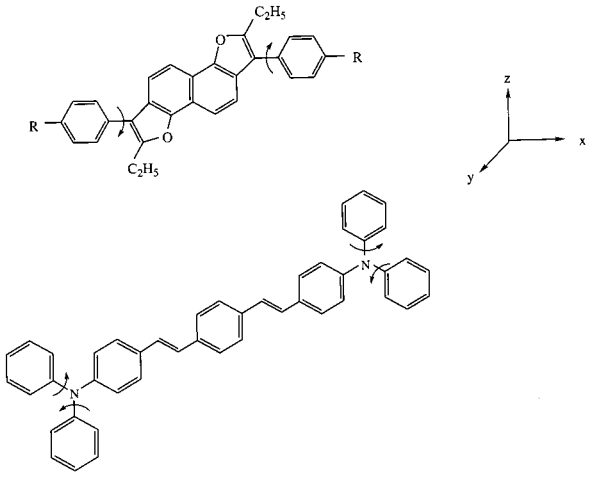

Figure 1. Diagrams illustrating the twist angle used as a variable in the computations on compounds **1(H)**, **1(CN)**, **1(CHO)**, and **5(H)**. The phenyl groups on opposing ends of the molecule were twisted such as to preserve a center of inversion in the molecule at all times which, in turn, facilitated computational ease.

performed over all intermediate states, including the ground state ($|k\rangle = |0\rangle$). Assuming incident radiation that is monochromatic and linearly polarized, the two-photon cross section for the $|0\rangle \rightarrow |f\rangle$ transition, δ_{0f}, can be expressed in terms of the two-photon matrix elements, $S_{\alpha,\beta}$, as shown in eq 2, where the summation is performed over the molecular axes *x*, *y*, and *z*.[14,33]

$$\delta_{0f} = \frac{1}{30}\sum_{\alpha,\beta}(2S_{\alpha,\alpha}S^*_{\beta,\beta} + 4S_{\alpha,\beta}S^*_{\beta,\alpha}) \qquad (2)$$

The standard split-valence, 3-21G, and split-valence plus polarization, 6-31G*, basis sets were used for most of the calculations. We also performed a few calculations with the larger 6-311G** basis set that contains extra diffuse and extra polarization functions. However, the results obtained were very similar to those obtained using the 6-31G* basis set, indicating that, at this level, inclusion of these extra basis functions had only a small effect on the two-photon cross section. Ideally, it is desirable to use even larger, more flexible basis sets to calculate nonlinear properties such as a two-photon cross section. However, this is simply not tractable given the size of the molecules in our study.

Prior to using the DALTON package, each of the geometric structures was optimized with the semiempirical PM3 method in the GAUSSIAN 98 program.[34] In calculations on **5(H)**, the geometries were also optimized with the semiempirical AM1 method in GAUSSIAN 98 and the results compared with those obtained using the PM3 method. For the study in which the dihedral angle of the pedant phenyl moieties in **1(H)**, **1(CN)**, and **1(CHO)** was changed, we took the optimized geometry and then simply twisted about the bond connecting the phenyl group to the difuranonaphthyl core (Figure 1).

Conversion to Experimental Units and the Band Shape Function. To compare the calculated two-photon cross sections, δ_{0f}, which are obtained in atomic units, with experimental data, it is necessary to have a cross section with the units cm^4 s $photon^{-1}$ (the so-called Göppert-Mayer units). Although this transformation of units has been achieved in a number of different ways by different investigators, a common problem is the need to quantify the spectral profile of the two-photon transition. For the moment, we will simply introduce a nondescript band shape function, $g(\nu)$, to describe the latter. Having done this, the transformation to a cross section in Göppert-Mayer units, σ_{0f}, can be achieved as shown in eq 3,[13,22,35] where the photon energy, ω, is known accurately and α is the fine structure constant [$\alpha = e^2/(4\pi\epsilon_0\hbar c)$].

$$\sigma_{0f} = \frac{(2\pi e)^4}{(4\pi\epsilon_0)^2 c^2 h^2} g(\nu)\omega^2\delta_{0f} = 4\pi^2\alpha^2 g(\nu)\omega^2\delta_{0f} \qquad (3)$$

Some investigators have used a variant of eq 3 in which $g(\nu)$ is divided by a damping factor, Γ, that reflects the lifetime broadening of the final state in the transition.[19,20,22] It is of course expected that both $g(\nu)$ and Γ will vary from one molecule to the next and depend on a number of variables including vibronic structure, solvent, and temperature. Nevertheless, it appears to have become a common practice to propagate similar values of $g(\nu)$ and Γ from one system to the next. For example, a value of $\Gamma = 0.1$ eV, assigned in a study of some phenylene vinylene derivatives because it gave good agreement between calculated and experimental cross sections,[19,20] has been used in studies of other molecules.[22]

Clearly, assumptions made about the band shape function increase the uncertainty with which σ_{0f} can be determined. Nevertheless, the incorporation of molecule-dependent parameters into $g(\nu)$ certainly limits this uncertainty. In our case, we will assume that $g(\nu)$ for all of the molecules studied herein can be represented as a Gaussian profile centered at the calculated frequency maximum for the final state, ν_f (eq 4).[13,14]

$$g(\nu) = g_{max}\exp\left(\frac{-4\ln 2}{(\Delta\nu)^2}(2\nu - \nu_f)^2\right) \qquad (4)$$

where $\Delta\nu$ is the full width at half-maximum of the given band. Since $g(\nu)$ is normalized in frequency space (i.e., $\int g(\nu)\, d\nu = 1$),

$$g_{max} = \left(\frac{4\ln 2}{\pi(\Delta\nu)^2}\right)^{1/2} = \frac{0.939}{\Delta\nu} \qquad (5)$$

Consequently, for a given two-photon absorption bandwidth, the maximum value of $g(\nu)$ will equal g_{max} and will have the units of seconds.

From the two-photon absorption spectrum of **1(CN)**,[5] we estimate a full width at half-maximum, $\Delta\nu$, of $\sim$1130 cm^{-1}, which, in turn, yields a g_{max} value of 2.77×10^{-14} s. Given the similarities between the molecules shown in Chart 1, we assume that this maximum value of $g(\nu)$ will be appropriate for all the difuranonaphthalenes studied. From the two-photon absorption spectrum of **5(Br)**,[5] we estimate a full width at half-maximum, $\Delta\nu$, of $\sim$1440 cm^{-1}, which yields a g_{max} value of 2.18×10^{-14} s. Given the similarities between the molecules shown in Chart 2, we assume that this maximum value of $g(\nu)$ will likewise be appropriate for the distyryl benzenes studied.

Other Sources of Computational Uncertainty and Error. It should be further noted that, although a large uncertainty is associated with the transformation to Göppert-Mayer units, our calculated cross sections are expected nevertheless to indicate a lower limit for the cross section we would observe experimentally. The principal origins for this expectation are twofold. First, in our calculations, we do not include electron correlation. As documented in other studies,[36,37] this limitation is generally manifested with computed hyperpolarizabilities that are smaller than those obtained using correlated electronic structure methods. In turn, the latter generally better represent experimental data. Second, our computations correspond to gas-phase conditions, whereas the experimental data are recorded

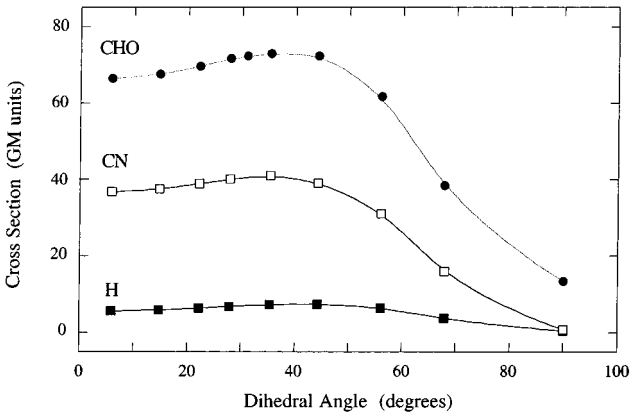

Figure 2. Plot of the calculated two-photon absorption cross section against the dihedral angle θ (see Figure 1) for compounds **1(H)**, **1-(CN)**, and **1(CHO)**. Calculations shown here were performed using the 6-31G* basis set. The cross sections are reported in Göppert-Mayer, GM, units (10^{-50} cm^4 s photon^{-1}).

in solution. Of course, there are many factors that can contribute to a discrepancy between gas and solution phase cross sections. For example, given constraints in DALTON, our computations are equivalent to the consideration of only a single vibronic transition. On the other hand, solution-phase experimental data will likely reflect several vibronic transitions that, in turn, should result in a larger cross section. Despite such differences between gas- and solution-phase systems, however, it has recently been reported in a computational study that, at least for some dipolar "push−pull" molecules embedded in a modeled solvent environment, the discrepancy between the respective two-photon cross sections may not actually be that large.[23] If it is assumed that the conclusions from this latter study are equally applicable to our molecules, one would only expect a two-photon cross section recorded in toluene to be ∼20−30% larger than that in the gas phase. It should also be noted that in converting our computational results to Göppert-Mayer units (eq 3), we use a band shape function derived from solution phase data. Thus, in principle, this factor should help mitigate the expected difference between the computational results and experimental data.

Results and Discussion

Difuranonaphthalenes. The substituted difuranonaphthalenes synthesized for our experiments were made with pendant *n*-octyl groups to facilitate solubility in toluene. To facilitate computational ease, the calculations were performed on analogues in which ethyl groups replaced the *n*-octyl groups (Chart 1). It is assumed that this change will have a negligible effect on the absorption cross section.

The first calculations were performed to assess the influence of the dihedral angle, θ, between the pendant phenyl groups and the difuranonaphthalene core (Figure 1). It is expected that at small angles θ, where appreciable π overlap between the difuranonaphthyl core and the pendant phenyl groups could facilitate charge migration, one would obtain larger transition moments and, in turn, larger two-photon cross sections. At large angles θ, however, it is expected that disruption of the extended π system would adversely influence the magnitude of the two-photon cross sections. Using compounds **1(H)**, **1(CN)**, and **1-(CHO)**, two-photon cross sections were calculated at angles ranging from 5 to 90° using both the 3-21G and 6-31G* basis sets. The same angle-dependent behavior was observed for all three compounds and both basis sets (Figure 2). At small angles, the cross section increased slightly with θ reaching a maximum value at a dihedral angle of ∼35°. Thereafter, with further increases in θ and the concomitant decrease in π overlap in the molecule, the cross section indeed decreased dramatically. As expected, computations performed on the analogous compounds **2(H)** and **2(CN)**, in which the pendant phenyl group is held in place via a bridging ethylene unit, yielded results comparable to those obtained at small angles θ with **1(H)** and **1(CN)**. Crystallographic data obtained from compound **1(H)** indicate an actual dihedral angle of ∼45°.[29] Given the comparatively small differences in calculated cross sections at θ∼35° and θ∼45° (Figure 2), we thus assume it is appropriate to compare the maximum values of the computed two-photon cross sections of **1(H)**, **1(CN)**, and **1(CHO)** to experimental data.

Given the limitations and caveats outlined in the section on computational methods, it is clear that there is remarkably good agreement between the calculated cross sections and the experimental data recorded for compounds **1(H)**, **1(CN)**, and **1(CHO)** (Table 1). Unfortunately, compound **2** was sufficiently insoluble in toluene as to preclude the acquisition of experimental cross sections. The computations not only reproduce relative substituent-dependent changes well, they also yield reasonably accurate absolute cross sections. Moreover, results obtained using the 3-21G basis set agree quite well with those obtained using the 6-31G* basis set. Indeed, this agreement between the cross sections obtained using the different basis sets applies to all of the results shown in Table 1. One important consequence of this latter result is that it builds confidence in the validity of numbers obtained using the poor, but computationally more efficient, 3-21G basis set. Thus, for comparatively large molecules in this same series, where use of the 6-31G* basis set may be precluded, a certain amount of trust can be placed in the results of computations using the 3-21G basis set.

The limited results discussed thus far indicate that substituents R, which withdraw electron density from the difuranonaphthalene core, give rise to a larger two-photon absorption cross section than that observed when R = H. One might thus expect a decrease in the cross section upon replacement of the terminal substituent in **1(R)** with an electron-donating functional group. This is indeed the case as illustrated for the results on **1(OCH3)**. Moreover, and again as one might expect based simply on qualitative electron withdrawal/donation arguments, a meta-substituted carbonyl (i.e., compound **3**) does not cause as large an increase in the cross section as a para-substituted carbonyl or a para-substituted nitrile (i.e., compounds **1(CHO)** and **1(CN)**, respectively). This latter point is confirmed both experimentally and computationally (Table 1). With respect to **3**, it is likely that the experimental two-photon cross section reported in Table 1 is an upper limit to the true value. For this compound, residual one-photon absorption at the irradiation wavelengths may contribute to the singlet oxygen signal observed.

Components of the Two-Photon Cross Section. To provide more information about parameters that could influence the magnitude of the two-photon cross section in these difuranonaphthalenes, we set out to look at individual components in the sum-over-state expression (eq 1), even though the latter was not actually used to obtain the cross sections shown in Table 1. Using linear response calculations, we obtained transition moments, $\langle 0|\mu|k\rangle$, and excitation energies, ω_k, from the ground state to a given state *k*. From the double residues of the quadratic response functions, we obtained transition moments between the intermediate and final states, $\langle k|\mu|f\rangle$. We then examined individual components of the two-photon absorption matrix for a range of intermediate states *k*. The calculations were performed

TABLE 2: Selected Contributions, in Atomic Units, from the Sum-Over-States-Expression for One Component, S_{xx}, of the Two-Photon Absorption Matrix Using a Range of Intermediate States *k*

	1(CN) $\theta = 28°$ $\omega_f/2 = 0.09466$			**1(H)** $\theta = 28°$ $\omega_f/2 = 0.10128$			**1(H)** $\theta = 67°$ $\omega_f/2 = 0.11372$		
k	ω_k	term	sum of terms	ω_k	term	sum of terms	ω_k	term	sum of terms
1	.1742	−1.6	−1.6	.1745	−1.0	−1.0	.1762	−1.8	−1.8
2	.1837	−6.5	−8.1	.1841	7.9	6.9	.1858	8.4	6.6
3	.1944	−68.3	−76.4	.2099	22.2	29.1	.2263	−2.7	3.9
4	.2173	1.1	−75.3	.2230	3.8	32.9	.2301	−5.8	−1.9
5	.2229	29.4	−45.9	.2252	1.0	33.9	.2312	0.3	−1.6
6	.2407	0.3	−45.6	.2411	−4.0	29.9	.2442	2.6	1.0
7	.2414	−2.7	−48.3	.2582	−39.4	−9.5	.2619	−47.3	−46.3
8	.2447	−49.4	−97.7	.2760	20.9	11.4	.2872	28.3	−18.0
9	.2506	−0.2	−97.9	.2777	−0.2	11.2	.2887	7.7	−10.3
10	.2659	−2.7	−100.6	.3026	−9.4	1.8	.2998	0.0	−10.3
11	.2687	−0.2	−100.8	.3058	1.4	3.2	.3046	−0.1	−10.4
12	.2735	−3.5	−104.3	.3083	10.0	13.2	.3062	−2.2	−12.6
13	.2927	24.3	−80.0						
∞			−62.8			23.2			−16.2

using the 3-21G basis set on three compounds: **1(H)**, $\theta = 28°$; **1(H)**, $\theta = 67°$; **1(CN)**, $\theta = 28°$ (Table 2).

In these compounds, both the ground and final states are totally symmetric (i.e., gerade, *g*, symmetry). Thus, because of the one-photon selection rules, the intermediate or virtual states will be of *u*, ungerade, symmetry.[6] Since the molecules are rather large, we expect the excitation energies, ω_k, for the first several dipole-allowed $g \rightarrow u$ transitions to be very similar. This indeed turns out to be the case (Table 2). Furthermore, there are no resonant one-photon transitions in the neighborhood of the resonant two-photon absorption. That is, the first few intermediate states *k* are all close in energy to the final state *f* and the difference $\omega_k - \omega_f/2$ in eq 1 is comparatively large. Consequently, the denominator of eq 1 is almost constant for the first several terms in the summation, and the states that most influence the two-photon matrix elements do so as a consequence of the transition moments in the numerator of eq 1. In particular, the effect of changing the substituent R from a hydrogen (i.e., **1(H)**) to a cyano group (i.e., **1(CN)**) is principally manifested in the magnitude of the transition moment between the intermediate and final states ($k \rightarrow f$). This latter observation is consistent with results obtained from the semiempirical calculations of Albota et al.[20] and Rumi et al.[38] on substituted distyryl benzenes using a three-state model.

For these particular molecules, the absence of intermediate states *k* with an energy close to $\omega_f/2$ clearly points to a design strategy by which significant gains can be achieved in the magnitude of the two-photon cross section. As has been demonstrated in other systems,[39] and as is apparent from eq 1, decreasing the difference $\omega_k - \omega_f/2$ will have a significant effect that can potentially dominate associated structure-dependent changes in the magnitudes of the transition moments.

For this study on **1(H)** and **1(CN)**, the coordinate system was chosen such as to place the difuranonaphthalene core in the *xz* plane (Figure 1). The calculations indicate that the S_{xx} and S_{xz} elements dominate the two-photon absorption matrix. This observation is consistent with the results of our study on the influence of the dihedral angle θ (vide supra) in which the absorption cross section is seen to decrease as elements with *y*-character become pertinent. However, to illustrate a particular point, we choose here to focus only on the S_{xx} elements calculated for a range of intermediate states *k*. In Table 2, we show the contribution from individual states *k* to the sum-over-states expression as well as the sum for all states considered. We also show the value of S_{xx} for an infinitely large number of states *k*. It is clear from the data that even after the inclusion of twelve intermediate states *k*, we are not particularly close to converging on the value of S_{xx} obtained from an infinitely large number of states *k*. Thus, when using a traditional sum-over-states model,[19,20] one must obviously be cautious when considering two-photon matrix elements that have been obtained by summing over only a few intermediate states. With this caveat in mind, however, it is interesting to note that for the first two compounds considered in Table 2, **1(CN)** and **1(H)** at $\theta = 28°$, the first dominant contribution ($k = 3$) appears to adequately reflect the total response obtained from a sum over an infinite number of states; −68.3 au vs −62.8 au for **1(CN)** and 22.2 au vs 23.2 au for **1(H)**. This phenomenon has been discussed previously by Birge and Pierce in the context of work on linear polyenes[14] and forms the basis of methods by which a sum-over-states calculation can be simplified.[19,40] However, for the final compound considered in Table 2, **1(H)** at $\theta = 67°$, where all we have done is increase the dihedral angle of the pendant phenyl groups, it is clear that the appropriate cross section obtained from the sum over all states is no longer dominated by one intermediate state. Thus, this example not only illustrates the sensitivity of the system to conformational changes but also illustrates the advantage of using response theory as opposed to a traditional sum-over-states model.

Pyrene and Distyryl Benzenes. As another test of response theory, we thought it necessary to see if we could likewise successfully model the behavior of a compound that has a comparatively small two-photon absorption cross section. To this end, we examined pyrene and found that our computations indeed modeled the experimental data well (Table 1).

Finally, we felt it appropriate to assess if we could calculate, with equal success, two-photon cross sections for a class of molecules significantly different from the difuranonaphthalenes but that likewise had comparatively large cross sections. Obvious molecules to consider in this regard are the distyryl benzenes initially studied by Albota et al.,[20] particularly since we use one of these molecules, **5(Br)**, as a reference standard in our experimental studies.[5]

As shown in Table 1, and again given the limitations and caveats outlined in the section on computational methods, it is clear that our calculations can indeed model the comparatively large two-photon cross sections of the distyryl benzenes **5**. As an aside, we should be somewhat circumspect when considering the remarkable agreement between the experimental and calculated cross sections for **5(Br)** in that the inclusion of heavy atoms in the molecule can be problematic in these types of calculations and particularly with the poor 3-21G basis set.[41,42]

TABLE 3: Calculated Two-Photon Absorption Cross Sections, δ, and Excitation Energies, E, for the Distyryl Benzene 5(H)

	method[a]	E (eV)	δ ($\times 10^{-5}$ au)
present work	3-21G, PM3	4.81	1.76
	6-31G*, PM3	4.62	1.41
	6-31G, PM3	4.71	1.40
	6-31G, AM1 ($\theta = 35°$, optimal θ)	4.58	2.90
	6-31G, AM1 ($\theta = 25°$)	4.54	2.99
	6-31G, AM1 ($\theta = 45°$)	4.64	2.57
Wang et al.[24]	6-31G, AM1	4.58	3.95

[a] See discussion in text. The angles refer to the extent of phenyl twist in the $-NPh_2$ moiety (see Figure 1).

Recently, Wang et al.[24] have also used response theory to calculate the two-photon absorption cross sections for **5(H)**, and it is instructive to compare our respective results for this molecule (Table 3). This comparison is best made using results obtained directly in atomic units to avoid any differences in the uncertainties associated with the transformation to Göppert-Mayer units (vide supra). Using a geometry optimized with the semiempirical AM1 method (MOPAC) and a standard 6-31G basis set, Wang et al.[24] found that the dominant two-photon transition would populate a state 4.58 eV above the ground state with a cross section of 3.95×10^5 au. For geometries optimized using the PM3 method and using the 3-21G and 6-31G* basis sets (i.e., data in Table 1), our calculations yield cross sections for transitions at roughly the same energy that are a factor of $\sim$2.5 times smaller. To identify the origin of these discrepancies, we performed a number of additional calculations (Table 3). Our principal finding is that the PM3 and AM1 methods yield different "optimal" geometries (i.e., they converge on different local minima on a multidimensional potential surface) that, in turn, give rise to different transition energies and cross sections. As expected, the salient features of these geometry differences involve the extent of twist about dihedral angles that disrupt π overlap. The latter include twisting the pendant phenyl groups in the $-NPh_2$ moiety (Figure 1, Table 3). For example, the PM3 method as well as the AM1 approach of Wang et al.[43] converge on a planar geometry for the distyryl benzene backbone. Alternatively, in our hands, the AM1 method (GAUSSIAN) converges on a twisted conformation for the distyryl benzene backbone.[44] These results on **5(H)** are consistent with those obtained on the difuranonaphthyl system shown in Figure 2 and illustrate the significant impact of molecular geometry and conformation on these nonlinear optical properties.

Wang et al.[24] have also compared the two-photon cross section for **5(H)** obtained using response theory to that obtained using a sum-over-states calculation in which only one dominant intermediate state k is considered. They find that, for this particular molecule and at their AM1 geometries, focusing solely on this single dominant state is sufficient to model the total response obtained from a sum over an infinite number of intermediate states. Thus, in this regard, **5(H)** behaves much like the first two difuranonaphthalenes considered in Table 2.

Predictions and the Synthesis of New Sensitizers. On the basis of the preceding results, we next wanted to see if we could use these computational tools to help design a difuranonaphthalene-based singlet oxygen sensitizer with a two-photon cross section that was larger than that, for example, of **1(CHO)**. To facilitate an increase in charge separation and thus influence the magnitude of the transition moments, it seemed reasonable to expect that extending the conjugation length of the molecule could be beneficial. Of course, we would still need to maintain electron-withdrawing substituents at the ends of the molecule as in **1(CN)** and **1(CHO)**. Given the success with which styryl units obviously connect electron-withdrawing and electron-donating moieties (i.e., compound **5**), it seemed reasonable to append styryl units to each end of our existing difuranonaphthyl core to generate a series of molecules denoted **4(R,R′)** (Chart 1). The decision to consider compound **4(CHO,CN)** was based on the results of an earlier, independent study in which we demonstrated that vinyl-substituted cyano groups dramatically increase the stability of phenylene vinylene oligomers (i.e., styryl benzenes) to photooxygenation.[45]

Two-photon cross sections calculated for **4(R,R′)** are shown in Table 1. The optimized geometry used for these calculations had a dihedral angle θ of 31° between the difuranonaphthyl core and the first phenyl of the pendant stilbenyl units. The phenyl rings in the latter were coplanar. As with the other molecules examined, the results obtained do not depend significantly on the basis set used. The calculations indicate that increasing the conjugation length alone (i.e., **4(H,H)**) does not appear to be sufficient to significantly impact the cross section. On the other hand, the computations indicate that the introduction of electron-withdrawing groups to the ends of the molecule (i.e., **4(CHO,H)**) should indeed give rise to a cross section larger than that seen in **1(CHO)**. Moreover, the computations indicate that a vinyl-substituted cyano group on the styryl link should not adversely influence the two-photon cross section.

With the preceding information in hand, we set out to synthesize some of these larger difuranonaphthyl systems and to experimentally quantify their two-photon absorption cross sections. The preparation of **4(CHO,H)** was most tractable and, upon comparison against **1(CHO)**, indeed yielded the comparatively large cross section of $(780 \pm 190) \times 10^{-50}$ cm^4 s photon^{-1} at 618 nm. This cross section was essentially independent of the irradiation wavelength over the range 615−680 nm, which is similar to the behavior observed from our other aldehyde-substituted difuranonaphthalene, **1(CHO)**, but contrasts with that observed from **1(CN)** where a distinct absorption band was recorded.[5]

As expected based on our earlier work with other substituted phenylene vinylenes,[45] **4(CHO,H)** was not as stable against photooxygenation as one might ideally desire (see Experimental Section). It is also clear from Table 1 that the singlet oxygen quantum yield from **4(CHO,H)** is not as large as one would ideally like. Thus, additional modifications of **4(R,R′)** at the molecular level must be considered to increase the quantum yield of triplet state production, for example, which, in turn, should have a significant effect on the singlet oxygen yield. The issues of sensitizer stability, efficiency, absorption profile, etc., demonstrate that the development of a suitable two-photon singlet oxygen precursor is indeed a complicated problem with many variables.

Conclusions

We have demonstrated that ab initio calculations using response theory can adequately model two-photon absorption cross sections for a series of comparatively large difuranonaphthalenes and distyryl benzenes. We have also demonstrated that the compounds examined in this study are viable two-photon singlet oxygen sensitizers. Thus, our results indicate that computational methods can indeed be a useful predictive tool in the design of molecules that could be used, for instance, as

agents for the treatment of cancers in photodynamic therapy and/or the creation of spatially resolved singlet oxygen images of heterogeneous samples.

Acknowledgment. This work was supported by grants from the Danish Research Council (Statens Naturvidenskabelige Forskningsråd, Materiale Forsknings Programmet) and the EU MOLPROP network. The authors thank Jan Thøgersen for useful discussions.

References and Notes

(1) Foote, C. S.; Clennan, E. L. In *Active Oxygen in Chemistry*; Foote, C. S., Valentine, J. S., Greenberg A., Liebman, J. F., Eds.; Chapman and Hall: London, 1995; pp 105−140.

(2) Ogilby, P. R.; Kristiansen, M.; Mártire, D. O.; Scurlock, R. D.; Taylor, V. L.; Clough, R. L. *Adv. Chem. Ser.* **1996**, *249*, 113−126.

(3) *Singlet Oxygen*; Frimer, A. A., Ed.; CRC Press: Boca Raton, 1985; Vol. I−IV.

(4) Wilkinson, F.; Helman, W. P.; Ross, A. B. *J. Phys. Chem. Ref. Data* **1993**, *22*, 113−262.

(5) Frederiksen, P. K.; Jørgensen, M.; Ogilby, P. R. *J. Am. Chem. Soc.* **2001**, *123*, 1215−1221.

(6) McClain, W. M. *Acc. Chem. Res.* **1974**, *7*, 129−135.

(7) Bhawalkar, J. D.; He, G. S.; Prasad, P. N. *Rep. Prog. Phys.* **1996**, *59*, 1041−1070.

(8) Xu, C.; Webb, W. W. In *Topics in Fluorescence Spectroscopy*; Lakowicz, J., Ed.; Plenum Press: New York, 1997; Vol. 5 Nonlinear and Two-Photon-Induced Fluorescence, pp 471−540.

(9) Fisher, W. G.; Partridge, W. P.; Dees, C.; Wachter, E. A. *Photochem. Photobiol.* **1997**, *66*, 141−155.

(10) Andersen, L. K.; Ogilby, P. R. *Photochem. Photobiol.* **2001**, *73*, 489−492.

(11) Fuchs, J.; Thiele, J. *Free Rad. Biol. Med.* **1998**, *24*, 835−847.

(12) Evleth, E. M.; Peticolas, W. L. *J. Chem. Phys.* **1964**, *41*, 1400−1407.

(13) Birge, R. R.; Bennett, J. A.; Pierce, B. M.; Thomas, T. M. *J. Am. Chem. Soc.* **1978**, *100*, 1533−1539.

(14) Birge, R. R.; Pierce, B. M. *J. Chem. Phys.* **1979**, *70*, 165−178.

(15) Karna, S. P.; Prasad, P. N. *J. Chem. Phys.* **1991**, *94*, 1171−1181.

(16) Lu, D.; Chen, G.; Perry, J. W.; Goddard, W. A. *J. Am. Chem. Soc.* **1994**, *116*, 10679−10685.

(17) Chen, G.; Lu, D.; Goddard, W. A. *J. Chem. Phys.* **1994**, *101*, 5860−5864.

(18) Barzoukas, M.; Blanchard-Desce, M. *J. Chem. Phys.* **2000**, *113*, 3951−3959.

(19) Kogej, T.; Beljonne, D.; Meyers, F.; Perry, J. W.; Marder, S. R.; Brédas, J. L. *Chem. Phys. Lett.* **1998**, *298*, 1−6.

(20) Albota, M.; Beljonne, D.; Brédas, J.-L.; Ehrlich, J. E.; Fu, J.-Y.; Heikal, A. A.; Hess, S. E.; Kogej, T.; Levin, M. D.; Marder, S. R.; McCord-Maughon, D.; Perry, J. W.; Röckel, H.; Rumi, M.; Subramaniam, G.; Webb, W. W.; Wu, X.-L.; Xu, C. *Science* **1998**, *281*, 1653−1656.

(21) Norman, P.; Luo, Y.; Ågren, H. *Chem. Phys. Lett.* **1998**, *296*, 8−18.

(22) Norman, P.; Luo, Y.; Ågren, H. *J. Chem. Phys.* **1999**, *111*, 7758−7765.

(23) Luo, Y.; Norman, P.; Macak, P.; Ågren, H. *J. Phys. Chem. A.* **2000**, *104*, 4718−4722.

(24) Wang, C.-K.; Macak, P.; Luo, Y.; Ågren, H. *J. Chem. Phys.* **2001**, *114*, 9813−9820.

(25) Sundholm, D.; Rizzo, A.; Jørgensen, P. *J. Chem. Phys.* **1994**, *101*, 4931−4935.

(26) Hättig, C.; Christiansen, O.; Jørgensen, P. *J. Chem. Phys.* **1998**, *108*, 8355−8359.

(27) Langhoff, S. R.; Davidson, E. R. *J. Chem. Phys.* **1976**, *64*, 4699−4710.

(28) Olsen, J.; Jørgensen, P. *J. Chem. Phys.* **1985**, *82*, 3235−3264.

(29) Jørgensen, M.; Krebs, F. C.; Bechgaard, K. *J. Org. Chem.* **2000**, *65*, 8783−8785.

(30) Kennedy, G.; Perboni, A. D. *Tetrahedron Lett.* **1996**, *37*, 7611−7614.

(31) Helgaker, T.; Jensen, H. J. A.; Jørgensen, P.; Olsen, J.; Ruud, K.; Ågren, H.; Bak, K. L.; Bakken, V.; Christiansen, O.; Dahle, P.; Dalskov, E. K.; Enevoldsen, T.; Fernandez, B.; Heiberg, H.; Hettema, H.; Jonsson, D.; Kirpekar, S.; Kobayashi, R.; Koch, H.; Mikkelsen, K. V.; Norman, P.; Packer, M. J.; Ruden, T. A.; Saue, T.; Sauer, S. P. A.; Sylvester-Hvid, K. O.; Taylor, P. R.; Vahtras, O. Dalton, an ab initio electronic structure program, Release 1.1 (July 2000). See http://www.kjemi.uio.no/software/dalton/dalton.html

(32) Shen, Y. R. *The Principles of Nonlinear Optics*; Wiley: New York, 1984.

(33) McClain, W. M. *J. Chem. Phys.* **1971**, *55*, 2789−2796.

(34) Frisch, M. J.; Trucks, W.; Schlegel, H. B.; Scuseria, G. E.; Robb, M. A.; Cheeseman, J. R.; Zakrezewski, V. G.; Montgomery, J. A.; Stratmann, R. E.; Burant, J. C.; Daprich, S.; Millam, J. M.; Daniels, A. D.; Kudin, K. N.; Strain, M. C.; Farkas, O.; Tomasi, J.; Baraone, V.; Cossi, M.; Cammi, R.; Menucci, B.; Pomelli, C.; Adamo, C.; Clifford, S.; Ochterski, J.; Peterson, G. A.; Ayala, P. Y.; Cui, Q.; Morokuma, K.; Malick, D. K.; Rabuck, A. D.; Raghavachari, K.; Cioslowski, J. B. F.; Ortiz, J. V.; Stefanov, B. B.; Jiu, G.; Liashenko, A.; Piskorz, P.; Komaromi, I.; Gomperts, R.; Martin, R. L.; Fox, D. J.; Keith, T.; Al-Laham, M. A.; Peng, C.-Y.; Nanayakkara, A.; Gonzalez, C.; Challacombe, M.; Gill, P. M. W.; Johnson, B. G.; Chen, W.; Wong, M.; Andres, J. L.; Head-Gordon, M.; Repolgle, E. S.; Pople, J. A. *Gaussian 98*; Gaussian Inc.: Pittsburgh, PA, 1998.

(35) Peticolas, W. L. *Annu. Rev. Phys. Chem.* **1967**, *18*, 233−260.

(36) Mikkelsen, K. V.; Luo, Y.; Ågren, H.; Jørgensen, P. *J. Chem. Phys.* **1995**, *102*, 9362−9367.

(37) Sylvester-Hvid, K. O.; Mikkelsen, K. V.; Jonsson, D.; Norman, P.; Ågren, H. *J. Chem. Phys.* **1998**, *109*, 5576−5584.

(38) Rumi, M.; Ehrlich, J. E.; Heikal, A. A.; Perry, J. W.; Barlow, S.; Hu, Z.; McCord-Maughon, D.; Parker, T. C.; Röckel, H.; Thayumanavan, S.; Marder, S. R.; Beljonne, D.; Brédas, J.-L. *J. Am. Chem. Soc.* **2000**, *122*, 9500−9510.

(39) Pati, S. K.; Marks, T. J.; Ratner, M. A. *J. Am. Chem. Soc.* **2001**, *123*, 7287−7291.

(40) Meyers, F.; Marder, S. R.; Pierce, B. M.; Brédas, J.-L. *J. Am. Chem. Soc.* **1994**, *116*, 10703−10714.

(41) Jensen, F. *Introduction to Computational Chemistry*; John Wiley and Sons: Chichester, 1999.

(42) Hehre, W. J.; Radom, L.; Pople, J. A.; Schleyer, P. v. R. *Ab Initio Molecular Orbital Theory*; Wiley: New York, 1986.

(43) Wang, C.-K.; Macak, P.; Luo, Y.; Ågren, H., private communication.

(44) With respect to the plane of the central ring in the three ring system of **5(H)**, (1) the planes of the bridging ethylene units define dihedral angles of 20°, twisted in opposite directions to maintain the center of inversion in the molecule, and (2) the planes of the outer rings define dihedral angles of 5°, again twisted such as to maintain the inversion center. A corollary of the preceding is that the planes of the outer rings and the bridging ethylene units define an angle of 15°.

(45) Dam, N.; Scurlock, R. D.; Wang, B.; Ma, L.; Sundahl, M.; Ogilby, P. R. *Chem. Mater.* **1999**, *11*, 1302−1305.

(46) Redmond, R. W.; Braslavsky, S. E. *Chem. Phys. Lett.* **1988**, *148*, 523−529.

(47) Kershaw, S. In *Characterization Techniques and Tabulations for Organic Nonlinear Optical Materials*; Kuzyk, M. G., Dirk, C. W., Eds.; Marcel Dekker: New York, 1998; pp 515−654.